

Encoding properties of the wing hinge stretch receptor in the hawkmoth *Manduca sexta*

Mark A. Frye

University of Washington, Department of Zoology, Box 351800, Seattle, WA 98195-1800, USA

Present address: Department of Integrative Biology, University of California, Berkeley, CA 94720, USA
(e-mail: markfrye@socrates.berkeley.edu)

Accepted 8 August 2001

Summary

To characterize the *in vivo* responses of the wing hinge stretch receptor of *Manduca sexta*, I recorded its activity and simultaneously tracked the up-and-down motion of the wing while the hawkmoth flew tethered in a wind tunnel. The stretch receptor fires a high-frequency burst of spikes near each dorsal stroke reversal. The onset of the burst is tightly tuned to a set-point in wing elevation, and the number of spikes contained within the burst encodes the maximal degree of wing elevation during the stroke. In an effort to characterize its mechanical encoding properties, I constructed an actuator that delivered deformations to the wing hinge and simultaneously recorded the resultant stretch and tension and the activity of the stretch receptor. Stimuli included stepwise changes in length as well as more

natural dynamic deformation that was measured *in vivo*. Step changes in length reveal that the stretch receptor encodes the static amplitude of stretch with both phasic and tonic firing dynamics. *In vivo* sinusoidal deformation revealed (i) that the timing of stretch receptor activity is tightly phase-locked within the oscillation cycle, (ii) that the number of spikes per burst is inversely related to oscillation frequency and (iii) that the instantaneous frequency of the burst increases with oscillation rate. At all oscillation rates tested, the instantaneous frequency of the burst increases with amplitude.

Key words: insect, flight, mechanosensory, proprioception, hawkmoth, *Manduca sexta*.

Introduction

For flight, both theoretical and experimental analyses show that wing deformation (Combes and Daniel, 2001) as well as wingstroke amplitude and velocity and the timing of rotations at the end of each stroke cycle (Dickinson et al., 1999; Sane and Dickinson, 2001) determine the pattern of aerodynamic forces produced by the beating wings. These kinematics are encoded by mechanosensory organs that each exert a powerful influence on the temporal dynamics of the flight motor pattern. In flies (Dickinson, 1990b), locusts (Elson, 1987b), and probably all insects, wing deformation during flight is encoded by campaniform sensilla arrayed across the wingblade. Afference from the campaniform organs of locust wings modulates the activity of flight interneurons and motoneurons (Elson, 1987a) and can entrain the flight rhythm (Horsmann and Wendler, 1985). In the locust, a stretch receptor inserts at the base of each wing and fires a burst of spikes near the top of the wingstroke (Möhl, 1985) encoding kinematic information such as the amplitude and timing of wing elevation. A good deal is known about the locust stretch receptor, such as the profile of its extensive afferent projections within the central nervous system (Altman and Tyrer, 1977), its specific synaptic connections with flight motoneurons (Burrows, 1975), its phasic influence on patterned motoneuron activity (Pearson et al., 1983) and its response to trapezoidal

deformation of its supporting tissue (Pfau et al., 1989). In locusts, its influence on the control of flight is powerful: it is able to both entrain and reset the flight rhythm (Reye and Pearson, 1988). As yet, we do not know whether the wing hinge stretch receptor plays a role in flight control across insect taxa, whether its feedback is used to modulate flight forces in response to visual cues [the subject of a companion study (Frye, 2001)] or how it encodes motions and forces acting on the wings.

The hawkmoth *Manduca sexta* is a deft aerial acrobat able to hover during feeding, mating and oviposition. The hawkmoth is a leading model system for the study of the kinematics and the resultant unsteady aerodynamics of flapping flight (Ellington, 1995; Willmott and Ellington, 1997a; Willmott and Ellington, 1997b). In *Manduca sexta*, ablation of stretch receptor feedback results in perturbed wing kinematics and decreased lift production in response to large-field visual cues during tethered flight (Frye, 2001). The importance of this proprioceptor to the flight system raises the general question of what kinds of wing motions and mechanical forces are encoded by the hawkmoth stretch receptor. In this paper, I describe stretch receptor activity in two preparations. In the first experiment, stretch receptor activity and wing motions were tracked simultaneously during

intact tethered flight in a wind tunnel to quantify those wing kinematics encoded by the stretch receptor. In the second experiment, the deformation of the stretch receptor during intact tethered flight was tracked using high-speed video. *In vivo* deformations were then delivered to the stretch receptor sensory apparatus in a reduced preparation to quantify the mechanical encoding properties of this proprioceptor.

Materials and methods

Recording stretch receptor activity and deformation in intact, tethered animals

Adult male and female *Manduca sexta* were reared on an artificial diet under a daily circadian photoperiod of 17h:7h L:D and were selected for experiments 3 days after adult eclosion. Moths were glued using cyanoacrylate adhesive to a rigid steel post between the metathoracic coxae. A small incision was made within the soft cuticle above the metathoracic axillary cord to expose the stretch receptor nerve (Fig. 1 inset). Nichrome wires (0.0254 mm diameter) insulated except at the tip (AM Systems Inc.) were formed into a single hook and reference electrode. The hook was placed around the stretch receptor nerve. The stretch receptor is tonically active at rest, so the quality of the recording was immediately evident. The recording site was insulated with either a drop of petroleum jelly diluted with mineral oil or a drop of non-toxic elastomer resin (Kwik Set) that polymerized into solid form soon after it was placed in the recording site. The electrode wires were fixed to the sclerotized scutum near the recording site and again on the dorsal scutellum with small drops of a molten 1:1 mixture of beeswax and rosin. The extracellular signal was a.c.-coupled and differentially amplified (4 ch. AM Systems, model 1800).

Tethered moths were mounted within an open-throat, closed-circuit wind tunnel constructed from tubular air-duct hose 11 cm in diameter. A computer fan mounted within the hose behind the moth powered the wind tunnel. An aluminum honeycomb section of aircraft flooring served as a flow straightener and was mounted at the opening of the wind tunnel in front of the tethered moth (Fig. 1). The windspeed, set at 1.5 m s^{-1} , was periodically monitored with a hot-wire anemometer (Kurz). *Manduca sexta* maintain a body angle of approximately 25° (the angle at which moths were tethered) at this windspeed (Willmott and Ellington, 1997a). Moths typically fanned their wings during a warm-up phase with low-amplitude wing motions for several minutes after the wind was turned on. Data were collected after the transition to normal flight.

The recording preparations were timed such that they were completed 1 h before the onset of the moth's subjective night. Moths were allowed to recover from the preparations and photoadapt to dark conditions at lights-out for at least one additional hour. Successful recordings generally did not last much more than 5 min after the transition from warm-up to full flight, by which time mechanical interference from the beating wings and contractions in the thorax destroyed the recording.

The vertical motion of one wing was tracked optically with a laser beam cast across the path of the wingstroke. A helium-neon laser was focused through both a cylinder lens and a collimating lens in series, which produced a two-dimensional 'sheet' of light. The laser sheet was focused along the longitudinal axis of the moth near the thorax such that the

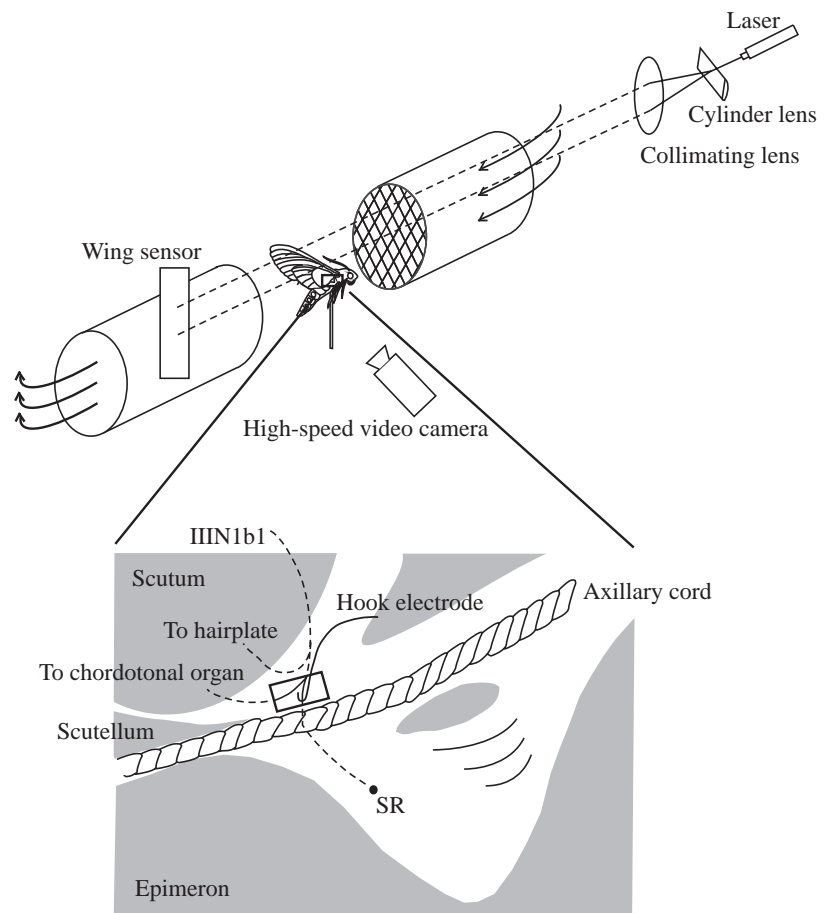


Fig. 1. Apparatus for recording extracellular stretch receptor activity during flight. Tethered moths were placed within a closed-circuit open-throat wind tunnel 11 cm in diameter. Windspeed was set at 1.5 m s^{-1} . A laser focused into a two-dimensional 'sheet' of light projected across the right wing, casting a shadow onto an optoelectronic sensor. The sensor circuit produced a voltage linearly proportional to the elevation of the wing. During flight, *in vivo* deformation of the subalar sclerite (with reference to the immobile epimeron) was tracked with a high-speed CCD camera fitted with a macro lens. The hindwing stretch receptor (SR, inset) sensory dendrites ramify within the soft membrane spanning the cuticle of the subalar sclerite and epimeron. A small incision (box) in the soft cuticle was made between the metathoracic scutum and hindwing axillary cord. The peripheral stretch receptor nerve was fixed in a hook electrode. The electrode and ground reference wires were glued to the scutum with a droplet of beeswax/rosin mixture.

wing transected the plane of light and cast a shadow on a 10 cm sensor (linear position detector; UDT Sensors Inc.) (Fig. 1). Transimpedance amplification circuitry was designed to track the shadow's centroid irrespective of its size. Therefore, the sensor produced a voltage linearly proportional to the vertical elevation of the wing irrespective of its angle of attack. I did not calibrate its output. During flight, moths occasionally exhibited what looked, to the naked eye, like attempts to steer. This behavior was characterized by strong abdominal ruddering and asymmetrical amplitudes of motion of the right and left wings. I only collected data for bouts in which the animal appeared to be maintaining a straight and level course. The amplified stretch receptor signal and voltage output from the wing position sensor were digitized at 10 kHz and stored on computer using a LabVIEW data-acquisition system running on a Macintosh PowerPC.

To aid in determining stretch receptor responses with respect to wing motions, I define two dimensionless parameters of wing kinematics for each wingstroke. The stretch receptor only produces action potentials as the wing is elevated towards the dorsal stroke reversal. Therefore, I quantify stretch receptor activity with respect to relative wing elevation instead of total wingstroke amplitude. Relative elevation was defined as the top position of each wingstroke (P_i) divided by the maximum position recorded (P_{max}) in volts (output of the wing sensor). I define the relative degree of wing elevation at the onset of the burst by dividing the position of the wing at the first spike (P_{sr}) by the maximum position recorded for that moth (P_{max}). For both measures, the lowest value of sensor voltage (corresponding to the ventralmost excursion of the wing) was subtracted from the entire recording before the ratios were calculated. Therefore, both measures ranged in value from 0 to 1.

Recording stretch receptor activity in response to controlled deformation of the stretch receptor sensory apparatus

In vivo deformations of the wing hinge were recorded during intact flight with a CCD camera (Redlake Motionscope), fitted with a macro lens, at $500 \text{ frames s}^{-1}$. The camera was oriented orthogonally to the long axis of the tethered moth (Fig. 1) such that the wing hinge occupied 80% of the field of view. The stretch receptor soma and dendrites insert within the soft cuticle of the metathoracic subalar membrane (Yack, 1992). The deformation of this soft tissue was tracked by referencing motion of the subalar sclerite to the immobile epimeron. Droplets of opaque white ink (WhiteOut) were applied to the base of the subalar sclerite and the top of the epimeron as reference markers. The two-dimensional (x,y plane) projection of the motion of the markers was digitized using mouseclick macros written in NIH Image v. 1.62. The deformation of the subalar membrane was contained primarily within the focal plane of the camera; out-of-plane motions were small. During flight, stretch amplitude roughly follows a sinusoid. Therefore, to estimate the mean frequency and amplitude of *in vivo* stretch, the time course of deformation was fitted to a sine function using a full Simplex minimization routine written in Matlab (v. 5.0).

To record stretch receptor activity, the legs and wings were amputated and the moth was glued to a steel post, which was bent into an L-shape to fit between the coxae. All six coxae were glued to the steel beam such that the sternal exoskeleton was completely immobilized. The right wing hinge and dorsal thorax were cleared of scales using compressed air and a small paintbrush. A mixture of low-melting-point beeswax and rosin was spread over the mesothorax and wing hinges to immobilize the thorax. Removing a portion of the metathoracic scutum exposed the stretch receptor nerve [see fig. 2 in Yack (Yack, 1992)], which was hooked with a stainless-steel recording electrode (Fig. 2, inset). A reference electrode was inserted in the hemolymph nearby. All experiments were conducted at an ambient temperature of 28°C .

A displacement actuator and force transducer were fashioned from the pen-motor assembly of a chart recorder (Gould 220). The pen motor uses a feedback circuit that delivers a current that minimizes the error between a command signal and the true rotation of the motor axle. Thus, the voltage produced by the feedback circuit is proportional to the torque

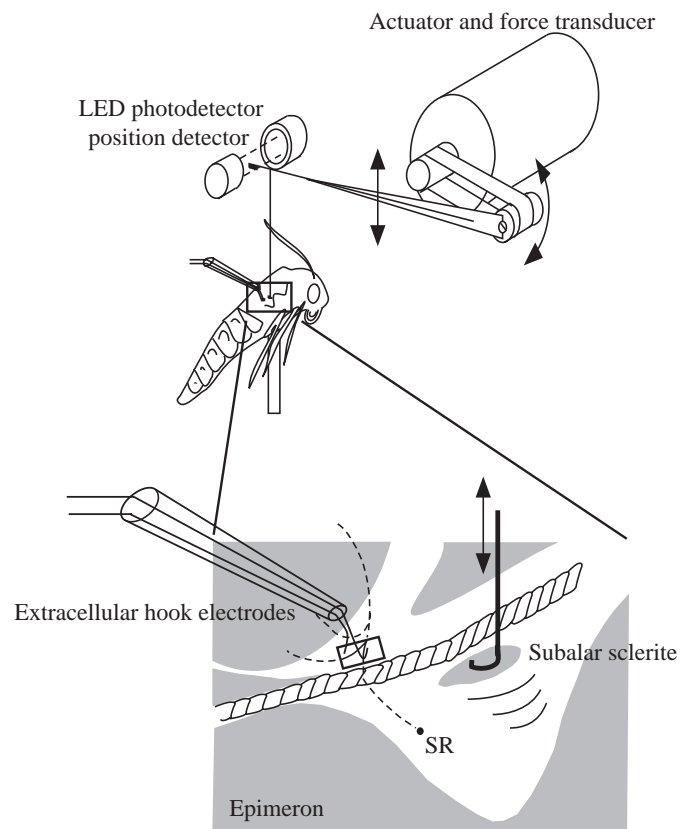


Fig. 2. Apparatus used to deliver controlled deformation to the stretch receptor (SR) and record subsequent extracellular activity. A chart recorder pen-motor was used as a stretch actuator and force transducer (see Materials and methods). An armature linked to the motor was glued to the subalar sclerite with cyanoacrylate adhesive. The stretch delivered to the tissue was tracked with an LED/photodetector pair, which produced a voltage linearly proportional to the position of the armature. Activity of the stretch receptor was recorded with a stainless-steel hook electrode.

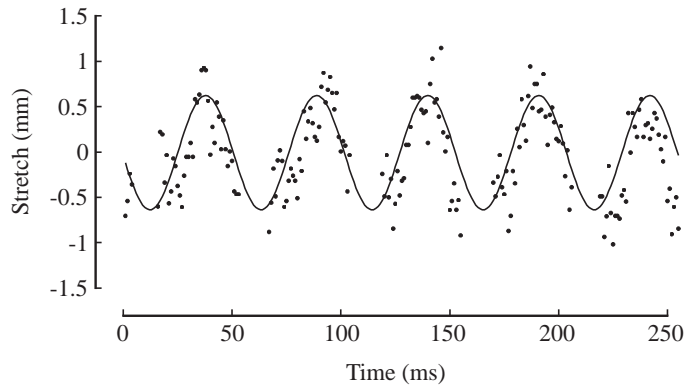


Fig. 3. *In vivo* deformation of stretch receptor tissue (subalar membrane). The locations of markers placed on the moving subalar sclerite and the immobile epimeron were recorded and digitized at $500 \text{ frames s}^{-1}$ during tethered flight. Filled symbols indicate the linear distance between the markers in successive video frames. A sine wave (solid line) was fitted to the data using a Simplex minimization routine written in Matlab (see Materials and methods). Note that there are periodic 'gaps' in the data series that correspond to times during which the downstroke of the wing occluded the view of the camera.

generated by the motor to position the pen. A brass armature was soldered to the pen assembly and fitted at the end with a small flag (Fig. 2). The position of the flag (thus the armature) was tracked with a light-emitting diode (LED) paired with an optical sensor (UDT Sensors Inc.). This entire assembly was mounted on a manual micromanipulator. The output of the position sensor tracked, with high precision, the stretch delivered to the subalar membrane by the actuator. The pen motor feedback signal was calibrated to force with static loads. During the experiments, peak excursion of the actuator assembly was $\pm 1 \text{ mm}$. The relationship between force and the voltage of the feedback circuit was linear over this range of displacement and had a slope of 0.0105 N V^{-1} .

A thin steel rod 1 cm in length was bent into a shallow hook and soldered to the end of the brass armature of the pen motor assembly. The hook was fixed to the subalar sclerite with a drop of cyanoacrylate adhesive before the stretch receptor recording electrodes were positioned (Fig. 2, inset). The output from a function generator (Hewlett Packard, model 3311A)

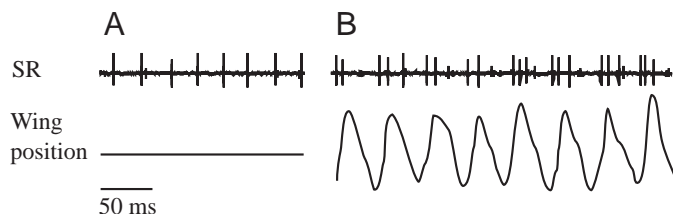


Fig. 4. Stretch receptor (SR) activity in tethered moths. At rest, the stretch receptor discharges tonically (A), and during flight it fires a phasic burst of spikes near the dorsal stroke reversal (B). The small unit active between stretch receptor bursts is cross-talk from a hindwing depressor muscle.

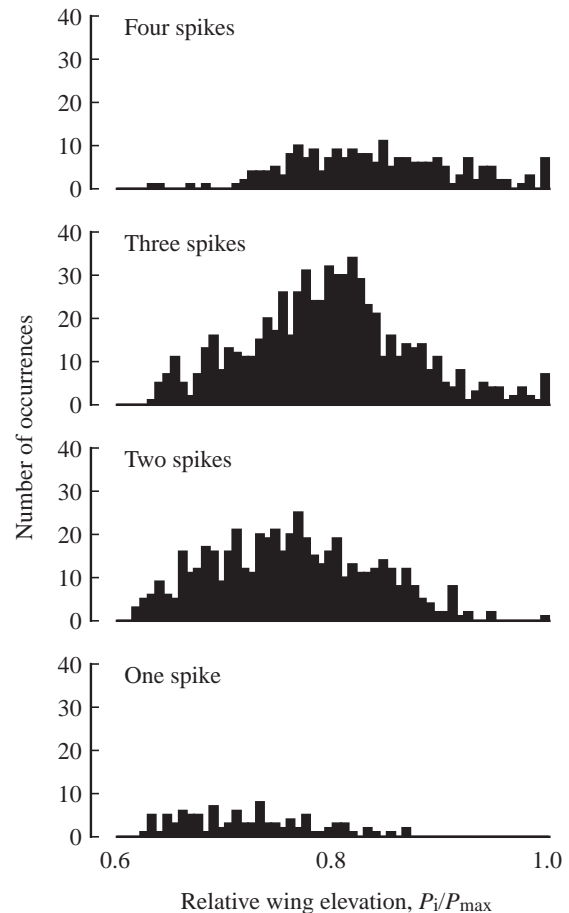


Fig. 5. During tethered flight, the number of spikes per stretch receptor burst increases with total wing elevation. Individual wingstrokes were segregated according to the number of stretch receptor spikes they evoked. Non-sequential histograms of relative wing elevation (see Materials and methods for definition) are plotted for bursts containing one, two, three or four spikes. While the distributions appear 'noisy', mean wing elevation increases significantly from 71 to 79% of maximal wing elevation (ANOVA, $F=85.7$, $P<0.001$). This data set comprises 1507 wing strokes from a single flight bout.

was used to drive the actuator assembly with square and sinusoidal waveforms. Voltage signals from the position sensor and the force transducer were lowpass-filtered at 100 kHz using an eight-pole Bessel filter (Underware Electronics). Outputs from the position sensor, force transducer and extracellular recording amplifier were digitized at 10 kHz and stored on computer using a LabVIEW data-acquisition system running on a Macintosh PowerPC.

Values in the text are presented as means \pm S.D.

Results

Wing hinge deformation, wing motions and stretch receptor activity during intact tethered flight

During tethered flight at a mean wingbeat frequency of 19.5 Hz, the mean displacement about resting length of the

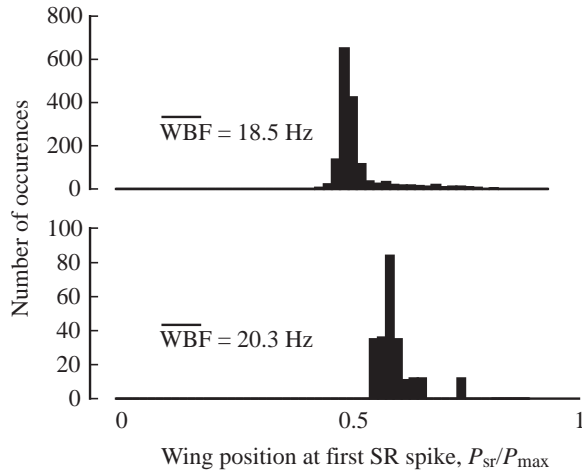


Fig. 6. The first stretch receptor (SR) spike is tightly tuned to the relative degree of wing elevation. Non-sequential histograms of wing position (see Materials and methods for definition) at the first stretch receptor spike are plotted for two moths with slightly different mean wingbeat frequencies (WBF, inset). The top histogram contains data from 1583 consecutive wingstrokes, and the lower histogram contains data from 206 consecutive wingstrokes.

stretch receptor supporting tissue was ± 0.6 mm (Fig. 3) corresponding to a displacement amplitude of 0.6 mm. Note that there are periodic ‘gaps’ in the data, which occur because the wing occludes the camera view of the wing hinge during

the downstroke. The strain axis relative to the body wall was measured *in vivo* and used to align the preparation properly during the *in vitro* experiments.

When the moth is quiescent the stretch receptor is spontaneously active at a frequency of 25 ± 1.3 Hz ($N=4$), while during flight it fires a burst of spikes near the top of each wingstroke (Fig. 4). By segregating individual wingstrokes according to the number of stretch receptor spikes evoked during each, I plotted a series of non-sequential histograms of relative elevation from a flight bout comprising 1507 wingstrokes (Fig. 5). Each plot represents the distribution of relative wing elevation for individual wing strokes where the stretch receptor fired one, two, three or four spikes within the stroke. Wing strokes for which the stretch receptor fired one, two, three or four spikes traveled on average 71 %, 74 %, 76 % or 79 %, respectively, through the maximum elevation (ANOVA, $P < 0.001$). Recordings from four moths yielded qualitatively similar results.

The stretch receptor burst begins near 50 % of the observed maximum wing elevation (Fig. 6). The first spike falls within a very narrow range of wing elevation. For one moth (Fig. 6, upper panel), the distribution is centered at 48 % of maximal wing elevation and the mean wingbeat frequency was 18.5 ± 1.2 Hz for 1583 consecutive wingstrokes. In the example from a second moth (Fig. 6, lower panel), the distribution is centered at 56 % of maximal wing elevation and the mean wingbeat frequency was 20.3 ± 0.7 Hz for 260 consecutive wingstrokes. Recordings from two other moths were similar,

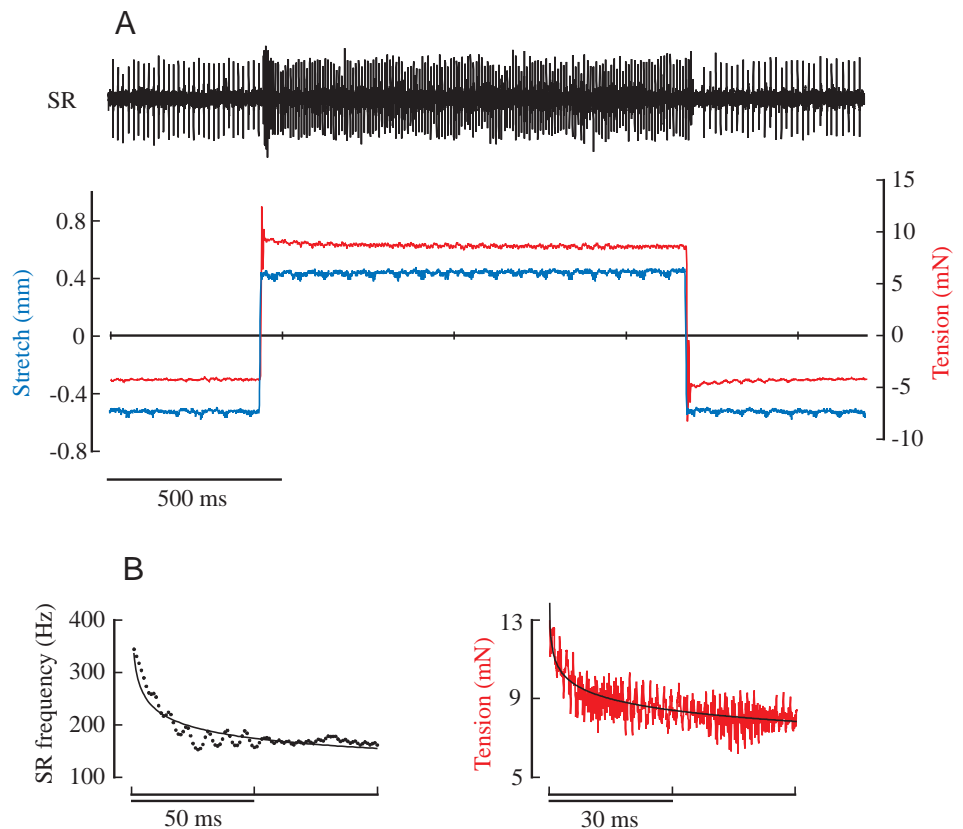


Fig. 7. Effects of stepwise deformation of the subalar membrane. (A) Tissue tension (red, right ordinate) and stretch receptor (SR) activity in response to square-wave steps in stretch (blue, left ordinate). In response to a rapid step in stretch, the stretch receptor produces a transient bout of high-frequency action potentials at the onset of the stretch, which declines rapidly to a tonic firing rate. (B) Time axis expansion of stretch receptor and tension responses illustrating that both stretch receptor firing rate and tension decay after the onset of a step in stretch (each plot was fitted with fractional power functions).

and the results presented here represent the quantitative extremes exhibited in the four recordings.

Stretch receptor responses to controlled deformation of the subalar membrane

I delivered both square-wave and sinusoidal oscillations in length (stretch) to the wing hinge. These patterns of deformation were delivered symmetrically about the resting length of the tissue. *In vivo*, the subalar membrane folds over itself during the downstroke and is stretched taut during the upstroke. Thus, positive values of stretch reflect deformation during an upstroke and *vice versa*. Tension in the subalar membrane exhibits partial stress-relaxation indicated by the decay in tension at constant stretch (Fig. 7A). At the onset of a 0.4 mm displacement, tension rises to 12.7 mN (maximum dynamic tension) and decays by 32% to a static level of 8.6 mN within 60 ms (Fig. 7B). A 'mirror-image' response in tension results from driving the tissue beyond its resting length (recorded as 'negative' tension). In this case, tension peaks at -9 mN and returns to approximately -4 mN within 60 ms.

The stretch receptor exhibits a phasicotonic response to stepwise displacement of the subalar membrane. At the onset of a step in stretch, mean firing frequency jumps to 350 Hz and decays by 51% to 170 Hz within 50 ms (Fig. 7A, time course expanded in Fig. 7B). Fig. 8 shows data from four moths indicated with different symbols; for a step magnitude of 0.97 mm, peak stretch receptor frequency decays from 350 to 150 Hz across animals (Fig. 8A). Instantaneous stretch receptor frequency during the initial phasic response increases linearly with increasing stretch amplitude (Fig. 8B, ANOVA, $P=0.03$). In other words, greater amplitudes of stretch evoke correspondingly stronger phasic responses. Stretch receptor frequency during the tonic component of its response also increases linearly with static stretch amplitude (Fig. 8C, ANOVA, $P=0.0002$). These results show that the stretch receptor encodes stretch magnitude with both phasic and tonic spiking dynamics.

In response to dynamic oscillation of the subalar membrane at frequencies and amplitudes bracketing the values observed *in vivo*, the stretch receptor fires a burst of spikes near peak stretch (Fig. 9). At an oscillation frequency of 5.4 Hz, the stretch receptor fires a burst of spikes that is loosely distributed within the cycle, although the most coherent group of spikes occurs slightly before peak stretch. As oscillation frequency is increased, the duration of the burst shortens and the burst becomes tightly phase-locked near the top of each stretch cycle.

The stretch receptor encodes the frequency, amplitude and timing of stretch oscillations. The number of spikes contained within the burst declines with increasing oscillation frequency, but does not vary significantly with changes in amplitude (Fig. 10A). Overall, the instantaneous frequency within the burst is strongly correlated with oscillation frequency (Fig. 10B, ANOVA, $P=0.0012$) and amplitude (Fig. 10B, ANOVA, $P=0.0143$). The degree of stretch at

which the burst is triggered also varies significantly with frequency (ANOVA, $P=0.0011$), but not with amplitude (Fig. 10C). The phase of the onset of the burst, with individual cycles defined by peaks in the stretch waveform, is tightly centered near -90° for all but the lowest oscillation frequency of 5.4 Hz (Fig. 10D; filled symbols). The end of the burst is tightly phase-locked near 0° (Fig. 10D; open symbols). Varying stretch amplitude has no significant effect on this phase-locking (Fig. 10D). Note that, for phase-locking to occur, the absolute timing of the burst varies as a function of oscillation frequency (Fig. 10D; inset).

The subalar muscle, which originates on the metathoracic epimeron, inserts on the subalar sclerite, so activity in this muscle could confound efforts to strictly control deformation of the subalar membrane. To be sure that the subalar muscle was not active during the experiments, I recorded electromyographic activity in the subalar muscle using a pair of nichrome wires implanted at the muscle insertion site. The muscle never produced suprathreshold potentials during the experiments while the moth was quiescent ($N=2$ data not shown).

Discussion

During tethered flight, the hawkmoth stretch receptor fires a burst of spikes near the top of each wingstroke (Fig. 4). The number of spikes per burst encodes the degree of wingstroke elevation (Fig. 5), and the onset of the burst is tightly phase-locked within the stroke cycle (Fig. 6). The stretch receptor sensory organ responds to step changes in tissue stretch with a phasicotonic modulation in frequency that is linearly proportional to stretch amplitude (Fig. 7, Fig. 8). In response to dynamic oscillations bracketing parameter values measured *in vivo*, the stretch receptor simultaneously encodes oscillation frequency and amplitude while remaining tightly phase-locked within the stretch cycle. These results suggest a complex viscoelastic coupling between deformation in the wing hinge, the resulting tension and the encoding dynamics of the stretch receptor.

Encoding properties of wing hinge stretch receptors

Electrophysiological responses of the wing hinge stretch receptors to wing elevation were originally reported for locusts (Gettrup, 1962) and have more recently been reported for several families of Lepidoptera (Yack and Fullard, 1993). This suggests that they may be common across insect taxa, although there is no direct evidence suggesting evolutionary homology between the locust and hawkmoth stretch receptors. During tethered flight in both locusts (Möhl, 1985) and *Manduca sexta*, the number of spikes contained in the stretch receptor burst corresponds to the degree of elevation in the wingstroke (Fig. 5). In the hawkmoth, there is also a critical threshold in wing elevation that triggers a burst of spikes (Fig. 6). While only qualitatively examined, it seems clear that the locust stretch receptor also encodes the degree of wing elevation in the number of spikes per burst and encodes wingbeat frequency

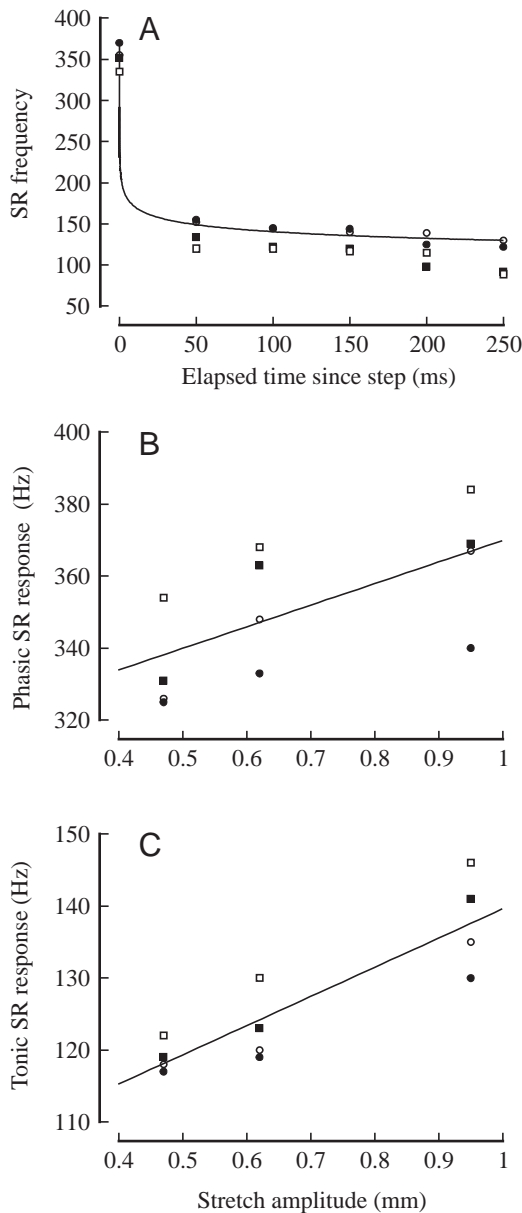


Fig. 8. Stretch receptor (SR) responses to stepwise stretch for four moths (different symbols). (A) The stretch receptor response consists of an early high-frequency phasic burst, which rapidly decays to a sustained tonic discharge (50 ms bins, fitted to a fractional power function). (B) Firing rate during the early phasic response *versus* stretch amplitude (linear regression, $r^2=0.41$; ANOVA, $F=6.9$, $P=0.03$). (C) Firing rate during the sustained tonic discharge *versus* stretch amplitude (linear regression, $r^2=0.8$; ANOVA, $F=32.6$, $P=0.0002$).

in the instantaneous frequency of the burst [see fig. 12a,b in Möhl (Möhl, 1985)].

The stretch receptor encodes the amplitude of displacement in the number of spikes and the instantaneous frequency of the burst in response to controlled mechanical displacement of the subalar membrane (Fig. 8, Fig. 10). In response to experimental oscillation of the entire wing in several species

of hawkmoth (Yack and Fullard, 1993) and in locusts (Burrows, 1975), stretch receptor firing rate is proportional to wing elevation. With increasing oscillation frequency, the number of spikes within the stretch receptor burst decreases, while the instantaneous frequency of spikes increases (Fig. 10A,B). The phase of the burst within the cycle does not vary with either amplitude or frequency (Fig. 10D). Thus, wing hinge stretch receptors signal the onset of, interval between and amplitude of wing elevations on a cycle-by-cycle basis during flight.

Passive tissue mechanics and encoding properties of mechanoreceptors

Spiking responses and adaptation in mechanosensory neurons emerge from complex interactions among (i) the mechanical coupling of the sensory neuron to its substratum, (ii) mechanochemical transduction at the level of deforming ion channels and (iii) the encoding properties of the spike initiating zone [for reviews, see Loewenstein (Loewenstein, 1971)]. In response to rapid steps in mechanical wing elevation, Gettrup (Gettrup, 1962) showed that the locust stretch receptor fires a phasic burst of spikes that adapts within approximately 25 ms to a tonic firing rate proportional to the degree of wing elevation. However Pfau et al. (Pfau et al., 1989) found no such phasic response during slower trapezoidal deformations (i.e. a ramp increase in amplitude, instead of a step) of the sensory apparatus and suggest that the stretch receptor encodes only static length, not its temporal derivatives. This discrepancy suggests that the sensory neuron, its supporting tissues or the linkage between the wing hinge and the wing itself contain non-linearities in their mechanical properties.

The stretch receptor in *Manduca sexta* is embedded in the subalar membrane (Yack, 1992). If this tissue were purely elastic, then tension would be directly proportional to stretch. Instead, tension in the subalar membrane exhibits stress-relaxation in response to stepwise stretch (Fig. 7). Also, if the subalar membrane were purely elastic, tension would follow stretch without any offset in phase during sinusoidal deformation. Instead, tension is phase-advanced at all frequencies and all amplitudes tested (Fig. 9, one representative amplitude shown). These behaviors indicate that the supporting tissue of the wing hinge stretch receptor displays both displacement-dependent elastic rebound and time-dependent viscous damping.

The stretch receptor also responds to a step in stretch in a manner similar to a standard viscoelastic solid. In time, the stretch receptor adapts to a tonic firing rate as the subalar membrane relaxes (Fig. 7B, Fig. 8A), albeit with a separate time course. Other stretch receptors, most notably the vertebrate muscle spindle and the crustacean intramuscular stretch receptor, exhibit both phasic and tonic spiking responses. The stretch receptor in *Manduca sexta* encodes the amplitude of a stepwise stretch (Fig. 8B) in its initial phasic burst as well as the static amplitude of the stretch (Fig. 8C) in its tonic discharge. The muscle spindle organ (Ottoson and

Shepherd, 1971) and crayfish stretch receptor (Terzuolo and Knox, 1971) exhibit qualitatively identical responses to steps in stretch. The relaxation in firing rate common to these mechanoreceptors has both mechanical and electrical bases, and the wing hinge stretch receptor deserves further investigation to dissociate the contributions of passive membrane dynamics, ion channel kinetics and encoding properties to the final output of the cell.

A morphological trait unique to the stretch receptor of the insect wing hinge is that it is not arranged in parallel with muscles. Thus, it cannot directly encode a muscle length change; instead, it encodes passive deformation of the wing hinge. During flight, wing hinge deformation is directly coupled with the internal forces associated with flight muscle contractions as well as the external aerodynamic and inertial forces acting on the wing. Therefore, the stretch receptor signal contains information about forces acting on the wings by directly encoding deformation in the wing hinge. Campaniform sensilla also encode forces acting on insect appendages *via* strains in the exoskeleton (Pringle, 1938). The responses of campaniform organs have been implicated in the dynamic control of posture and locomotion in the cockroach (Ridgel et al., 2000) and of flight in flies (Dickinson, 1990a). Chapman et al. (Chapman et al., 1979) determined that passive mechanical properties alone cannot explain sensory adaptation to stepwise indentation of campaniform caps. They show that these biological strain gauges exhibit different rates of adaptation to force and indentation, suggesting that force is encoded separately from strain.

The stretch receptor encodes the timing and amplitude of wing elevations that are driven by internal and external forces acting on the wings. Stretch receptor feedback probably tunes the flight motor pattern such that individual wingstrokes are temporally precise and are of appropriate amplitude. These kinematic patterns, in turn, mediate aerodynamic moments in response to external mechanical perturbations such as turbulent wind and internal guidance or steering cues descending from the brain. Another intriguing hypothesis about the ultimate function of the stretch receptor signal emerges from the fact that insects do not simply beat their wings up and down as they fly. Each translation, during which the wing is held at a nearly constant angle of attack, is followed by pronation or supination, during

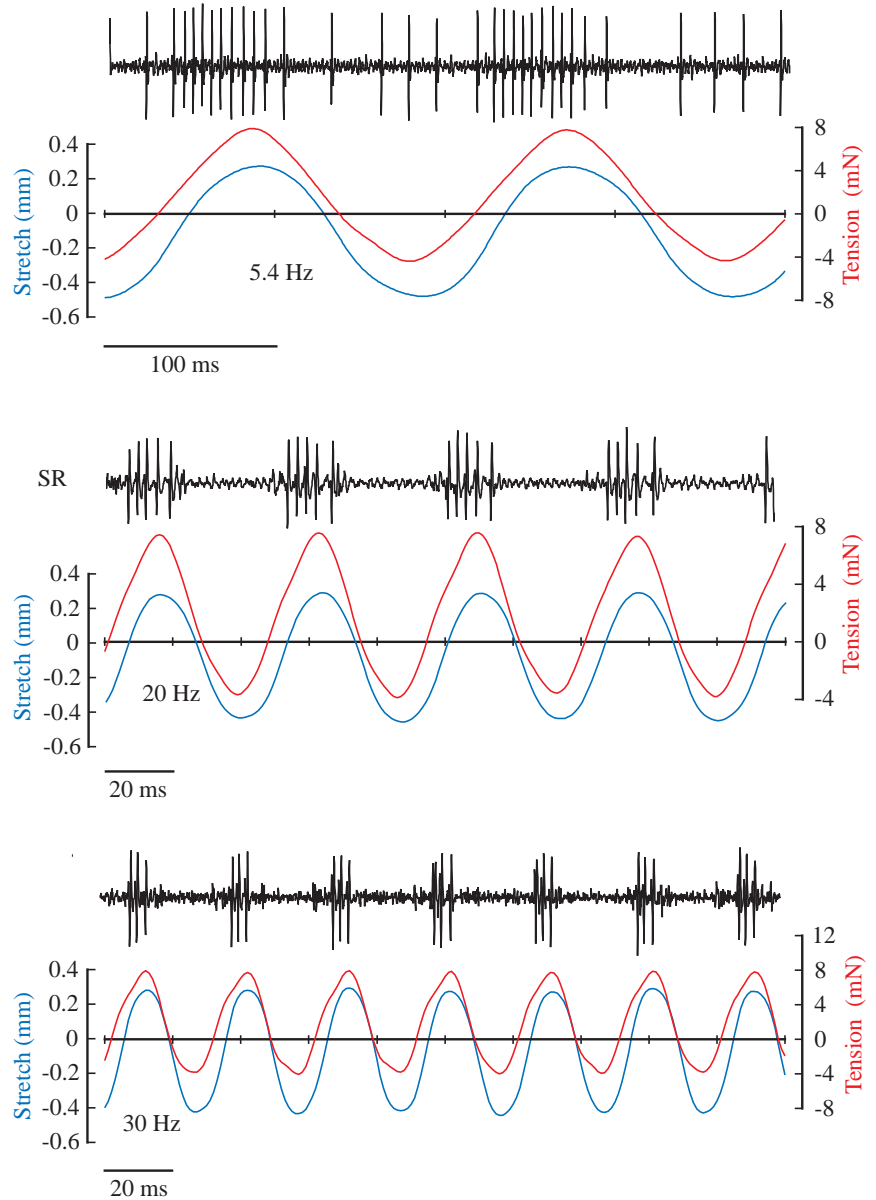


Fig. 9. Effects of deformation of the subalar membrane approximating *in vivo* conditions. Tension (red, right ordinate) and extracellular recording of stretch receptor activity (black) in response to sinusoidal stretch (blue, left ordinate) of the subalar membrane. Sample data are plotted for three oscillation frequencies indicated numerically within each plot.

which the wing is rotated about a spanwise axis. The timing of these rotations within the stroke cycle is a major determinant of unsteady aerodynamic force production in several species of fly (Sane and Dickinson, 2001) and possibly in all flying insects. The stretch receptor is certainly active during pronation at the top of the upstroke and responds to twisting of the wing (Pfau, 1983). It may encode the timing and magnitude of rotational kinematics during the upstroke, and this feedback may be used in the control of rotational kinematics by steering muscles and resultant aerodynamic force production.

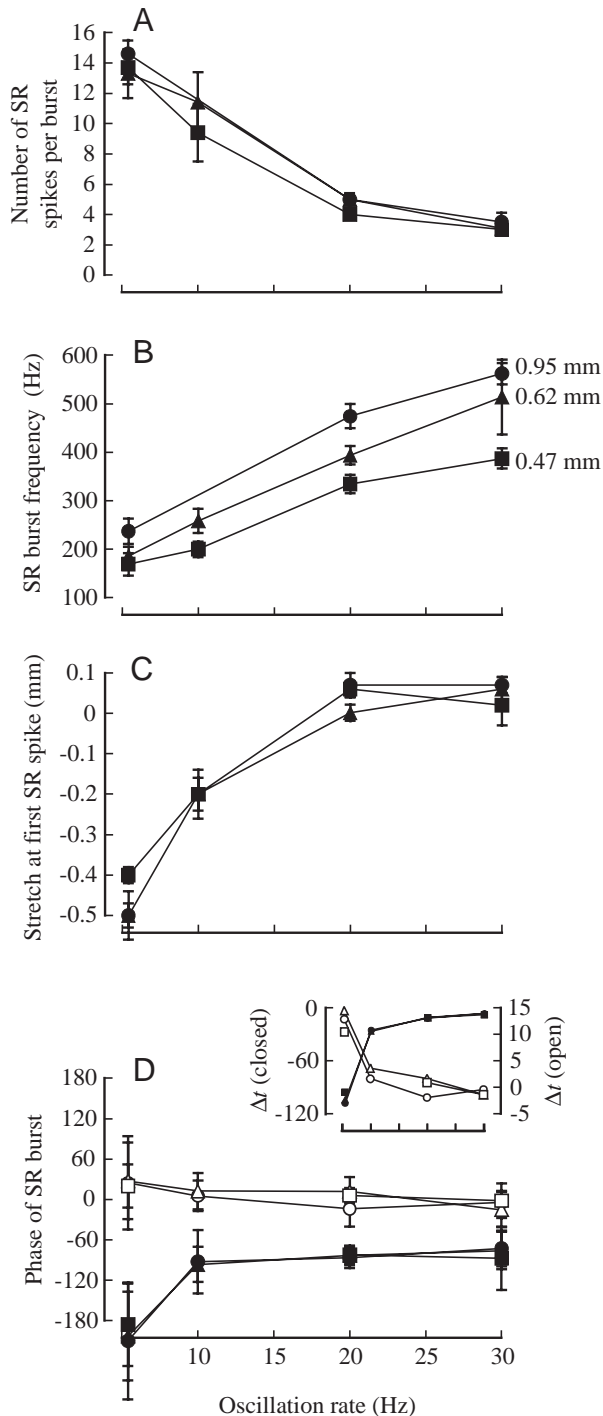


Fig. 10. Mean ($N=4$) stretch receptor (SR) responses to varying oscillation frequency and stretch amplitude. (A) Mean number of spikes per burst. (B) Mean stretch receptor firing rate (ANOVA, oscillation frequency, $F=12.2$, $P=0.0012$; amplitude, $F=6.6$, $P=0.14$). (C) Degree of stretch at the onset of the stretch receptor burst (ANOVA, oscillation frequency, $F=9.9$, $P=0.0073$). (D) Phase of stretch receptor burst with respect to peaks in the stretch waveform. The onset (termination) of a burst is indicated with filled (open) symbols. Different symbol shapes indicate the stretch amplitudes indicated numerically in B. Values are means \pm s.d. Inset: data from D replotted as the difference in time (Δt) between peaks in stretch and onset (termination) of the burst indicated with filled (open) symbols

I wish to thank Tom Daniel for his intellectual and technical support during this research. I thank J. W. Truman, M. S. Tu, D. C. O'Carroll and members of the Daniel, Truman and O'Carroll laboratories for thoughtful advice throughout the course of this project. I am also grateful for the valuable comments of two anonymous referees. The project was funded by NSF grant 9511681 to Tom Daniel and NIH Graduate Neuroscience Training Grant to M.A.F.

References

- Altman, J. S. and Tyrer, N. M. (1977). The locust wing hinge stretch receptors. I. Primary sensory neurons with enormous central arborizations. *J. Comp. Neurol.* **172**, 409–430.
- Burrows, M. (1975). Monosynaptic connexions between wing stretch receptors and flight motoneurons of the locust. *J. Exp. Biol.* **62**, 189–219.
- Chapman, K. M., Mosinger, J. L. and Duckrow, R. B. (1979). The role of distributed viscoelastic coupling in sensory adaptation in an insect mechanoreceptor. *J. Comp. Physiol.* **131**, 1–12.
- Combes, S. A. and Daniel, T. L. (2001). Shape, flapping and flexion: wing and fin design for forward flight. *J. Exp. Biol.* **204**, 2073–2086.
- Dickinson, M. H. (1990a). Linear and nonlinear encoding properties of an identified mechanoreceptor on the fly wing measured with mechanical noise stimuli. *J. Exp. Biol.* **151**, 219–244.
- Dickinson, M. H. (1990b). Comparison of encoding properties of campaniform sensilla on the fly wing. *J. Exp. Biol.* **151**, 245–261.
- Dickinson, M. H., Lehmann, F. O. and Sane, S. P. (1999). Wing rotation and the aerodynamic basis of insect flight [see comments]. *Science* **284**, 1954–1960.
- Ellington, C. P. (1995). Unsteady aerodynamics of insect flight. *Symp. Soc. Exp. Biol.* **49**, 109–129.
- Elson, R. C. (1987a). Flight motor neurone reflexes driven by strain-sensitive wing mechanoreceptors in the locust. *J. Comp. Physiol. A* **161**, 747–760.
- Elson, R. C. (1987b). Interneuronal processing of inputs from the campaniform sensilla of the locust hindwing. *J. Comp. Physiol. A* **161**, 761–776.
- Frye, M. A. (2001). Effects of stretch receptor ablation on the optomotor control of lift in the hawkmoth *Manduca sexta*. *J. Exp. Biol.* **204**, 3683–3691.
- Gettrup, E. (1962). Thoracic proprioceptors in the flight system of locusts. *Nature* **193**, 498–499.
- Horsmann, U. and Wendler, G. (1985). The role of a fast wing reflex in locust flight. In *Insect Locomotion* (ed. M. Gewecke and G. Wendler), pp. 157–165. Berlin: Paul Parey.
- Loewenstein, W. R. (ed.) (1971). *Handbook of Sensory Physiology*, vol. 1, *Principles of Receptor Physiology*. New York: Springer-Verlag.
- Möhl, B. (1985). The role of proprioception in locust flight control. II. Information signalled by forewing stretch receptors. *J. Comp. Physiol. A* **156**, 103–116.
- Ottoson, D. and Shepherd, G. M. (1971). Transducer properties and integrative mechanisms in the frog's muscle spindle. In *Handbook of Sensory Physiology*, vol. 1 (ed. W. R. Loewenstein), pp. 442–500. New York: Springer-Verlag.
- Pearson, K. G., Reye, D. N. and Robertson, R. M. (1983). Phase-dependent influences of wing stretch receptors on flight rhythm in the locust. *J. Neurophysiol.* **49**, 1168–1181.
- Pfau, H. K. (1983). Mechanik und sensorische Kontrolle der Flügel-Pronation und -Supination. In *BIONA-Report 1* (ed. W. Nachtigall), pp. 61–77. Stuttgart, New York: Akad. Wiss. Mainz: G. Fischer.
- Pfau, H. K., Koch, U. T. and Möhl, B. (1989). Temperature dependence and response characteristics of the isolated wing hinge stretch receptor in the locust. *J. Comp. Physiol. A* **165**, 247–252.
- Pringle, J. W. S. (1938). Proprioception in insects. II. The action of the campaniform sensilla on the legs. *J. Exp. Biol.* **15**, 114–131.
- Reye, D. N. and Pearson, K. G. (1988). Entrainment of the locust central flight oscillator by wing stretch receptor stimulation. *J. Comp. Physiol. A* **162**, 77–89.
- Ridgel, A. L., Frazier, S. F., DiCaprio, R. A. and Zill, S. N. (2000). Encoding of forces by cockroach tibial campaniform sensilla: implications

- in dynamic control of posture and locomotion. *J. Comp. Physiol. A* **186**, 359–374.
- Sane, S. P. and Dickinson, M. H.** (2001). The control of flight force by a flapping wing: lift and drag production. *J. Exp. Biol.* **204**, 2607–2626.
- Terzuolo, C. A. and Knox, C. K.** (1971). Static and dynamic behavior of the stretch receptor organ of Crustacea. In *Handbook of Sensory Physiology*, vol. 1 (ed. W. R. Loewenstein), pp. 500–523. New York: Springer-Verlag.
- Willmott, A. P. and Ellington, C. P.** (1997a). The mechanics of flight in the hawkmoth *Manduca sexta*. I. Kinematics of hovering and forward flight. *J. Exp. Biol.* **200**, 2705–2722.
- Willmott, A. P. and Ellington, C. P.** (1997b). The mechanics of flight in the hawkmoth *Manduca sexta*. II. Aerodynamic consequences of kinematic and morphological variation. *J. Exp. Biol.* **200**, 2723–2745.
- Yack, J. E.** (1992). A multiterminal stretch receptor, chordotonal organ and hair plate at the wing-hinge of *Manduca sexta*: unravelling the mystery of the noctuid moth ear b cell. *J. Comp. Neurol.* **324**, 500–508.
- Yack, J. E. and Fullard, J. H.** (1993). Proprioceptive activity of the wing-hinge stretch receptor in *Manduca sexta* and other atympanate moths: a study of the noctuid moth ear B cell homologue. *J. Comp. Physiol. A* **173**, 301–307.